Genomics Proteomics Bioinformatics

www.elsevier.com/locate/gpb
www.sciencedirect.com

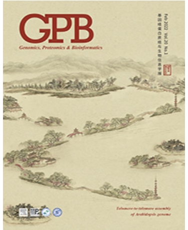

ORIGINAL RESEARCH

Resequencing 250 Soybean Accessions: New Insights into Genes Associated with Agronomic Traits and Genetic Networks

Chunming Yang[1,#], Jun Yan[2,#], Shuqin Jiang[2], Xia Li[3], Haowei Min[4,*], Xiangfeng Wang[2,*], Dongyun Hao[1,*]

[1] *Key Laboratory for Agricultural Biotechnology of Jilin Provincial, Institute of Agricultural Biotechnology, Jilin Academy of Agricultural Sciences (JAAS), Jilin 130033, China*
[2] *Frontiers Science Center for Molecular Design Breeding, College of Agronomy and Biotechnology, China Agricultural University, Beijing 100094, China*
[3] *Key Laboratory of Molecular Cytogenetics and Genetic Breeding of Heilongjiang Province, College of Life Science and Technology, Harbin Normal University, Harbin 150025, China*
[4] *BioTrust Technology Inc., Beijing 100094, China*

Received 13 December 2020; accepted 6 March 2021
Available online 24 July 2021

Handled by Peng Cui

KEYWORDS

Agronomic trait;
GWAS;
Network;
Resequence;
Soybean

Abstract The limited knowledge of genomic diversity and functional genes associated with the traits of **soybean** varieties has resulted in slow progress in breeding. In this study, we sequenced the genomes of 250 soybean landraces and cultivars from China, America, and Europe, and investigated their population structure, genetic diversity and architecture, and the selective sweep regions of these accessions. Five novel agronomically important genes were identified, and the effects of functional mutations in respective genes were examined. The candidate genes *GSTT1*, *GL3*, and *GSTL3* associated with the isoflavone content, *CKX3* associated with yield traits, and *CYP85A2* associated with both architecture and yield traits were found. The phenotype–gene **network** analysis revealed that hub nodes play a crucial role in complex phenotypic associations. This study describes novel agronomic trait-associated genes and a complex genetic network, providing a valuable resource for future soybean molecular breeding.

Introduction

Soybean *Glycine max* [L.] Merr. is one of the most important crops worldwide, serving as a vegetable oil and protein source for human and livestock feed. Soybean originated in China, and its wild species (*G. soja* Sieb. & Zucc.) was domesticated

[*] Corresponding authors.
E-mail: dyhao@cjaas.com (Hao D), xwang@cau.edu.cn (Wang X), biotrust_st@163.com (Min H).
[#] Equal contribution.

Peer review under responsibility of Beijing Institute of Genomics, Chinese Academy of Sciences / China National Center for Bioinformation and Genetics Society of China.

https://doi.org/10.1016/j.gpb.2021.02.009
1672-0229 © 2022 The Authors. Published by Elsevier B.V. and Science Press on behalf of Beijing Institute of Genomics, Chinese Academy of Sciences / China National Center for Bioinformation and Genetics Society of China.
This is an open access article under the CC BY-NC-ND license (http://creativecommons.org/licenses/by-nc-nd/4.0/).

in approximately 3000 BC before being introduced into Korea and Japan about 3000 years later. It was brought to Europe and North America in the 18th century and cultivated globally since the 19th century [1].

With the rapid development of modern molecular biology and high-throughput sequencing technologies, whole-genome resequencing and genome-wide association studies (GWAS) have become common methods to study population genetic diversity and locate phenotype-related quantitative trait loci (QTLs) or genes. These methods have significantly improved our knowledge of crop genomes and selective breeding. In recent years, an increasing number of reports have been published on the domestication and improvement of soybean at the genome-wide level. These include genes and genetic networks related to agronomic traits and functions of soybean [2–4]. However, our knowledge of the soybean genome and its functional genes is still limited compared to rice and maize [5–7], which is attributed to the diversity of soybean varieties and their complex genetic backgrounds. Therefore, a large number of soybean varieties need to be further explored at the genomic level, particularly in relation to molecular traits associated with edible quality, ideal plant architecture, and the underlying genetic network of high-yielding varieties.

In this study, 250 soybean accessions were collected from the core Northeast China soybean germplasm pool, consisting of 134 accessions of landraces and cultivars from Northeast and Northwest China and 116 accessions from European and North American cultivars. The genomes of most of these accessions were not sequenced previously. The high-depth whole-genome resequencing and comprehensive analyses of these 250 soybean accessions were performed. The resulting dataset revealed valuable information on soybean genome structure, novel genes associated with important agronomic traits, and genetic networks. These genetic resources provide unique references for further exploring molecular breeding and evolution in soybean.

Results

Genotyping of 250 diverse soybean accessions by genome resequencing

High-depth whole-genome resequencing was performed on 250 soybean accessions, including 51 landraces and 83 cultivars originating from provinces in Northeast China (*i.e.*, Heilongjiang, Jilin, Liaoning, and Inner Mongolia) and Northwest China (*i.e.*, Xinjiang, Ningxia, and Gansu), as well as 116 cultivars originating from Europe and North America (Table S1). Approximately 10 gigabyte (GB) / 3 tera-basepair (Tb) of pair-end reads were obtained. The maximum sequencing depth of a single accession was 22.5×, with an average depth of 11×. After filtering out the raw sequencing data (see Materials and methods), the remaining high-quality cleaned data were compared with the soybean reference genome *G. max* v2.0 [8]. The effective mapping rates ranged from 74.8% to 87.6%, while the genome coverages ranged from 94.8% to 97.0% (Table S1). The high mapping rates and high coverages guaranteed that the sequencing data are reliable and high-quality.

A total of 6,333,721 single-nucleotide polymorphisms (SNPs) and 2,565,797 insertions and deletions (InDels) were detected through standard variation detection, genotype filtering, and imputation steps (see Materials and methods). This included 244,360 SNPs and 62,714 InDels located in exon regions. The ratio of nonsynonymous to synonymous SNP substitutions was 1.37. Furthermore, we found 4,311,814 SNPs with a minor allele frequency (MAF) larger than 0.05 (Figure S1; Table S3). In summary, more than 6 megabyte (MB) high-density and high-quality genotype data were obtained from 250 soybean accessions with a density of 1 SNP every 15 bases.

Population structure analysis of 250 soybean landraces and cultivars

Using the 6 MB SNP genotype dataset, a phylogenetic tree was constructed using the neighbor-joining (NJ) method. As a result, the 250 soybean accessions were classified into 4 groups (**Figure 1**A). Group 1 comprised 65 Chinese, 4 European, and 6 American varieties; Group 2 comprised 56 Chinese, 1 European, and 13 American varieties; Group 3 comprised 21 European, 2 Chinese, and 6 American cultivars; Group 4 comprised 65 American cultivars and 11 Chinese varieties (Figure 1B). A Bayesian clustering algorithm based on a mixed model was used to estimate the proportion of ancestors in each accession. When $K = 2$, the main ancestor component (yellow) of Group 4 was split, indicating that Group 4 had the highest level of selection. When $K = 3$, the main ancestor component (blue) of Group 3 was split, indicating that Group 3 had the second level of selection. However, when $K = 4$ and $K = 5$, Groups 1 and 2 exhibited complex differentiated mixed ancestor components, indicating the higher genetic diversities and lower selection levels in Groups 1 and 2 (Figure 1C; Table S3).

The results of the principal component analysis (PCA) were consistent with those of the phylogenetic tree. Three groups, Groups 1, 3, and 4, radiated away from Group 2 within the rectangular coordinate system projected using eigenvector 1 and eigenvector 2 data on the *x*-axis and *y*-axis, respectively. Concurrently, the distribution of varieties in the four groups showed continuity, indicating that the varieties located in different groups also had genetic similarities (Figure 1D).

These results indicated that the group classification of the 250 soybean accessions was closely related to their geographical distribution. That is, varieties with similar geographical distribution had similar genetic backgrounds. Generally speaking, the group classification was also related to the level of domestication. Landraces had a lower level of domestication, while cultivars had higher levels of domestication. Varieties with similar domestication levels tended to have a higher similarity in genetic backgrounds. However, still, differences were found in the geographical distribution and domestication level among breeds with similar genetic backgrounds, indicating that gene exchange might have occurred between accessions of different groups. This observation reflected the complexity of soybean domestication history.

Genetic diversity and selective sweep analysis for soybean subpopulations

We next performed a linkage disequilibrium (LD) analysis. The results showed that the overall LD decay distance was more than 100 kb, and the LD decay distance of the landraces

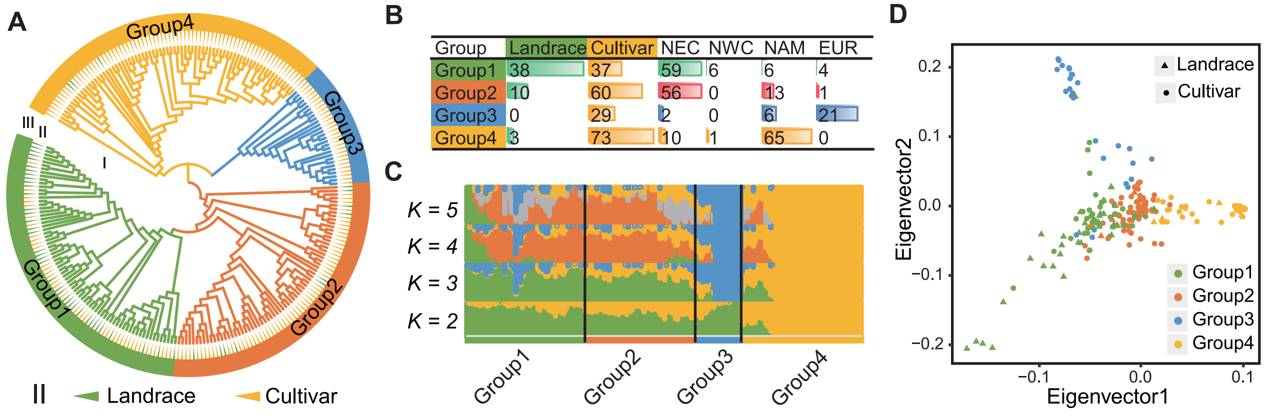

Group	Landrace	Cultivar	NEC	NWC	NAM	EUR
Group1	38	37	59	6	6	4
Group2	10	60	56	0	13	1
Group3	0	29	2	0	6	21
Group4	3	73	10	1	65	0

Figure 1 Population structure analysis of 250 soybean landraces and cultivars

A. Phylogenetic tree constructed for all soybean accessions. Groups 1–4 are shown with different colors, landraces are labeled with green triangles, and cultivars are labeled with yellow triangles. **B.** Statistics of the geographic origin for each subpopulation. **C.** Mixed ancestor analysis for soybean subpopulations. Each color represents an ancestral component. *K* from 2 to 5 is set to trace different ancestral components. **D.** Principal component analysis plot of the first two eigenvectors for all soybean accessions. Landraces and cultivars are shown with different shapes, while groups are shown with different colors. NEC, Northeast China; NWC, Northwest China; NAM, North America; EUR, Europe.

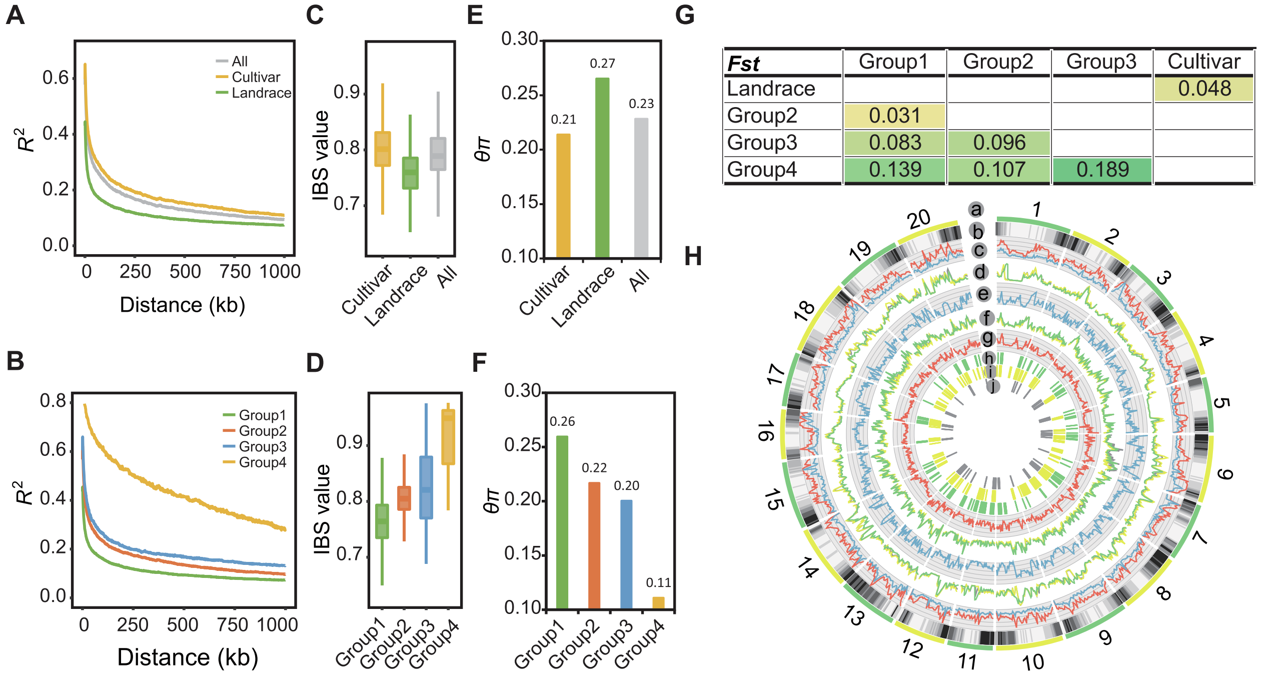

Fst	Group1	Group2	Group3	Cultivar
Landrace				0.048
Group2	0.031			
Group3	0.083	0.096		
Group4	0.139	0.107	0.189	

Figure 2 Genetic diversity analysis and putative selective regions of soybean subpopulations

A. LD decay plots for landraces (green), cultivars (yellow), and all soybean accessions (gray). **B.** LD decay plots for soybean subpopulations. **C.** IBS value distribution for landraces (green), cultivars (yellow), and all soybean accessions (gray). **D.** IBS value distribution for soybean subpopulations. **E.** Comparison of $\theta\pi$ values for landraces (green), cultivars (yellow), and all soybean accessions (gray). **F.** Comparison of $\theta\pi$ values for soybean subpopulations. **G.** Comparison of *Fst* values between landraces and cultivars and between subpopulations. **H.** Landscape of soybean genetic diversity across the whole genome. (a) Chromosomes. (b) Density of genes. (c) Density of SNPs (red) and InDels (blue). (d) LD value distribution for landraces (green), cultivars (yellow), and all accessions (gray). (e) *Fst* value distribution of landraces *versus* cultivars. (f) $\theta\pi$ value distribution for landraces (green), cultivars (yellow), and all accessions (gray). (g) Tajima's *D* value distribution of all accessions. (h) Putative selective sweep regions detected by Tajima's *D* combined with $\theta\pi$. (i) Putative selective sweep regions detected by *Fst* combined with $\theta\pi$ ratios. (j) ROH region larger than 300 kb. LD, linkage disequilibrium; IBS, identical-by-state; SNP, single-nucleotide polymorphism; InDel, insertion and deletion; ROH, runs of homozygosity.

was smaller than that of the cultivars (**Figure 2**A). Further LD decay analysis of the four groups showed that the LD decay distance in Group 1 was the smallest, followed by Groups 2 and 3, while Group 4 had the largest LD decay distance (Figure 2B). In addition, the LD levels varied for different chromosomes or different regions across one chromosome. An identical-by-state (IBS) analysis, which reflects the degree of relatedness among individuals by calculating the consistency of all genetic markers, revealed that the average IBS value of landraces was less than that of cultivars (Figure 2C). The IBS values of Groups 1–4 followed the same trends as the LD decay distances. In particular, the IBS values of Group 1 were the lowest, and those of Group 4 were the highest among all groups (Figure 2D). $\theta\pi$ values reflect the genetic diversity within a population by calculating the number of different sites between any two sequences or individuals within a population. *Fst* is a calculation used to measure the differentiation and genetic distance between two populations. $\theta\pi$ values were calculated for landraces, cultivars, all accessions, and Groups 1–4. *Fst* values were calculated between landraces and cultivars and between the four groups. The results showed that a population with a higher LD decay distance or higher IBS values was correlated with a smaller $\theta\pi$ (Figure 2E and F), indicating an opposite pattern to those of the LD decay distances and IBS values. The lowest *Fst* value was for Group 1 *versus* Group 2, while the highest *Fst* value was for Group 3 *versus* Group 4. Also, the *Fst* value of Group 2 *versus* Group 3 was higher than that of Group 1 *versus* Group 3 (Figure 2G). The *Fst* value of Group 2 *versus* Group 4 was smaller than that of Group 1 *versus* Group 4. In addition, the results of our allele frequency distribution (AFD) analysis, as an alternative population similarity measurement, were consistent with the *Fst* results (Figure S2). When combined with the population structure and geographical distribution information, the results of our population diversity analysis inferred that the European and American soybean varieties might have originated from different Chinese ancestors before undergoing independent selection. The results indicated that European cultivars and the Chinese landrace group (Group 1) had a more recent common ancestor, while North American cultivars and the Chinese cultivar group (Group 2) had a more recent common ancestor.

Tajima's *D* (based on a neutral test), $\theta\pi$ (based on genetic diversity within a population), and *Fst* (based on genetic diversity between two populations) are highly effective tools that can screen selective sweep signals across a genome [9]. These methods were combined in pairs for mining potential selective sweep regions in the soybean genome that might have undergone artificial selection. One pair was Tajima's *D* combined with $\theta\pi$ for the whole population. Another pair was *Fst* combined with $\theta\pi$ ratios between two subpopulations/landraces/cultivars. A sliding window method was used to calculate the values of Tajima's *D*, $\theta\pi$, and *Fst* in each window across the whole genome (Figure 2H), and the top 5% significant windows were selected as potential selective sweep regions (Figure S3A and B). A total of 148 and 222 potential selective sweep regions were screened by the aforementioned two combined methods, and they covered 36.09 Mb and 88.15 Mb genome regions, respectively (Table S4). These potential selective sweep regions covered 9128 genes, accounting for approximately one-sixth of all soybean genes. A total of 1876 genes were screened by both methods (Figure S3C). Runs of homozygosity (ROH) regions, continuous homozygous chromosome regions in a genome, may be related to domestication or artificial selection [10]. Through an ROH analysis, 71 ROH regions larger than 300 kb were obtained from all 250 accessions, with a total length of 27.84 Mb. The longest ROH region up to 911 kb was located at the beginning of chromosome 10 (Table S5). Furthermore, 3397 genes were located in these ROH regions, 924 of which were also located in the potential selected sweep regions (Figure S3D).

Identification of significantly associated loci and genes through GWAS of 50 agronomic traits

A total of 50 agronomic traits were measured in 250 soybean accessions from three geographic locations for three years and then integrated using the best linear unbiased prediction (BLUP). The 50 traits included traits related to architecture (15), color (5), isoflavone (1), oil (4), protein (18), and yield (7), and were classified into six categories (Table S6). Pearson correlation coefficients for traits were calculated to compare within and between categories, revealing that traits within the same category were more strongly correlated than traits in different categories. Specifically, strong positive or negative correlations were found between almost all traits within the protein-related, oil-related, and yield-related categories. For example, the linoleic acid content was positively correlated with the linolenic acid content but negatively correlated with the oleic acid content; stem intension was negatively correlated with lodging (Figure S4). Some traits were evenly distributed, while others were ranked (Figures S5–S54).

GWAS was performed on 4,311,814 SNPs with MAF > 0.05, using the mixed linear model (MLM) method for the aforementioned 50 agronomic traits. For each trait, a clump-based method [11] was used, and a significantly associated locus (SAL) in a chromosome region was defined with a substantial amount of SNPs associated with a specific trait. A total of 203 SALs were detected for 43 traits (Figures S5–S54; Table S7). Since each SAL may contain dozens of genes, a functional mutation-based haplotype test was used for further mining of the most reliable candidate trait-associated genes [12]. In particular, only the nonsynonymous SNPs, frameshift InDels, and mutations within a gene that happened on a start or stop codon, splice sites, or transcription start sites were considered as effective functional mutations. These mutations were used to classify each gene into different haplotypes, and the phenotypic differences of the accessions belonging to each haplotype were subsequently tested. A gene with significant phenotypic differences was defined as a significantly associated gene (SAG), and 3165 SAGs were thus screened for 43 traits. These SAGs included some QTLs or genes that were previously identified, such as the flower color-related chr13:16551728–19506795, pubescence color-related chr6:16930159–19168772, seed coat luster-related chr15:8910798–10281804, palmitic acid content-related chr5:879095–1682551 [4], isoflavone content-related chr5:38880530–39142565 [13], plant height-related *Dt1* [4], and oil content-related *FAD2* and *SAT1* [14]. These SAGs also contained genes that were identified for the first time in soybean, such as the isoflavone content-related *GL3* and glutathione S-transferase (GST) L3 (*GSTL3*), the yield trait-related cytokinin oxidase/dehydrogenase 3 (*CKX3*), and the architecture and yield trait-related *CYP85A2* (**Table 1**).

Table 1 Functional variants of representative significant associated genes

Variant ID	Chromosome	Positon	Reference	Alternative	Variant type	Gene ID	Gene symbol
c5s38936266	5	38,936,266	C	T	Nonsynonymous SNV	GLYMA_05G206900	*GSTT1a*
c5s38940717	5	38,940,717	C	T	Nonsynonymous SNV	GLYMA_05G207000	*GSTT1b*
c5s39035509	5	39,035,509	G	C	Nonsynonymous SNV	GLYMA_05G208300	*GL3*
c5s39036346	5	39,036,346	T	C	Nonsynonymous SNV	GLYMA_05G208300	*GL3*
c13s24804891	13	24,804,891	C	T	Nonsynonymous SNV	GLYMA_13G135600	*GSTL3*
c13s24805363	13	24,805,363	A	T	Splicing SNV	GLYMA_13G135600	*GSTL3*
c17s4143663	17	4,143,663	C	T	Nonsynonymous SNV	GLYMA_17G054500	*CKX3*
c17s4143832	17	4,143,832	T	C	Nonsynonymous SNV	GLYMA_17G054500	*CKX3*
c17s4146922	17	4,146,922	G	T	Nonsynonymous SNV	GLYMA_17G054500	*CKX3*
c17s4151713	17	4,151,713	C	A	Nonsynonymous SNV	GLYMA_17G054600	*CKX4*
c17s4151752	17	4,151,752	T	C	Nonsynonymous SNV	GLYMA_17G054600	*CKX4*
c18s55526062	18	55,526,062	C	T	Nonsynonymous SNV	GLYMA_18G272300	*CYP85A2*

Note: SNV, single nucleotide variant.

Association of GSTT1, GL3, and GSTL3 with the isoflavone content

The isoflavone content is an important quality-related trait in soybean, but its molecular mechanism is still unclear. This study identified four SALs related to the isoflavone content, namely chr3:38590023–38728718, chr5:3888053–39142565, chr13:18342836–18541809, and chr5:24726091–24852447. Only one SAL, chr5:24726091–24852447, overlapped with a previously reported QTL that contained a *GST* gene GST theta 1 (*GSTT1*) [13]. All the other SALs were newly identified. Furthermore, 48 genes were located within these SALs (Table S8), and three genes (*GSTT1*, *GL3*, and *GSTL3*) might be related to the isoflavone content (**Figure 3**A and B). Two functional mutations were present at c5s38936266 and c5s38940717, forming two haplotypes for *GSTT1a* and *GSTT1b*, respectively. For each *GSTT1* gene, soybean accessions with a different haplotype were related to significantly different isoflavone contents. Since *GSTT1a* and *GSTT1b* were approximately only 1 kb apart from each other in the same genome region, the two genes were considered to be one in the subsequent analysis. Three haplotypes were formed by two functional mutations when the two *GSTT1* genes were analyzed as one. Haplotype 1 *versus* Haplotype 2 and Haplotype 2 *versus* Haplotype 3, showed significant differences in the isoflavone content, while Haplotype 1 *versus* Haplotype 3 showed no significant difference (analyzed using Tukey's test). This finding suggested that *GSTT1a* was associated with the isoflavone content due to its linkage with *GSTT1b*. However, c5s38936266 did not contribute to the difference in the isoflavone content. Thus, only c5s38940717 on *GSTT1b* was associated with the isoflavone content (Figure 3C). Two functional mutations, c5s39035509 and c5s39036346, producing two haplotypes in *GL3*, were associated with different isoflavone contents in soybean accessions (Figure 3D). Also, another *GST* gene, *GSTL3*, was identified, which was located on chromosome 13. Two functional mutations within *GSTL3* produced three haplotypes, and significant associations between the different haplotypes and the isoflavone contents were detected for each comparison (Figure 3E). Based on these results, a schematic diagram of the roles of these three candidate genes was drawn according to their biological functions. The diagram indicates that *GL3* regulates isoflavone synthesis, while *GSTT1* and *GSTL3* participate in isoflavone transport (Figure 3F).

Association of CKX3 with yield-related traits and its location in an artificial selection region

Four yield-related traits (pod number per plant, seed number per plant, one hundred seed weight, and seed size) have a common SAL located in the region between ~ 4.0 Mb and ~ 4.2 Mb on chromosome 17 (**Figure 4**A). Further analyses revealed that this SAL contained two tandem repeat *CKX* genes named *CKX3* and *CKX4*, approximately 15 kb apart from each other (Figure 4B).

The relationship between functional mutations of *CKX3* and *CKX4* was further analyzed. Three and two nonsynonymous SNPs were located in *CKX3* and *CKX4*, respectively. As these two genes were only approximately 15 kb apart from each other in the same genomic region, the two genes were analyzed separately as well as combined as one in relation to their association with haplotypes and traits (Figure 4C–F). The results showed that the functional mutations could form either three haplotypes for each individual genes or four haplotypes for the *CKX 3 + 4* combined. For all comparisons in all traits, Haplotype 1 always showed significant differences compared with the other haplotypes. The relationship between different haplotypes in terms of pod or seed number per plant showed a consistent trend, while that in terms of one hundred seed weight or seed size showed a consistent but opposite trend. A phenotypic correlation was found between pod number per plant and seed number per plant (0.92) as well as between one hundred seed weight and seed size (0.67) (Figure 4G). Furthermore, we observed that *CKX3* and *CKX4* were located in different strands of the same chromosome, suggesting that they were more likely to have independent functions. However, the expression of *CKX4* was not detected in the subsequent qRT-PCR validation. Thus, only *CKX3* was regarded as a real candidate gene, while the role of *CKX4* needs further investigation.

When the soybean accession information of each haplotype for the four yield-related traits was compared, most accessions with the Haplotype 1 genotype had dominant traits (lower pod or seed numbers and larger seeds and seed weights) and were more associated with cultivars. The other haplotypes were mainly landrace-specific haplotypes, and their accessions all belonged to Group 1. *CKX3* was also located in a strong selective sweep region. This indicated that the functional mutation sites in *CKX3* experienced strong directed artificial selection, resulting in genotype differences and affecting yield-related

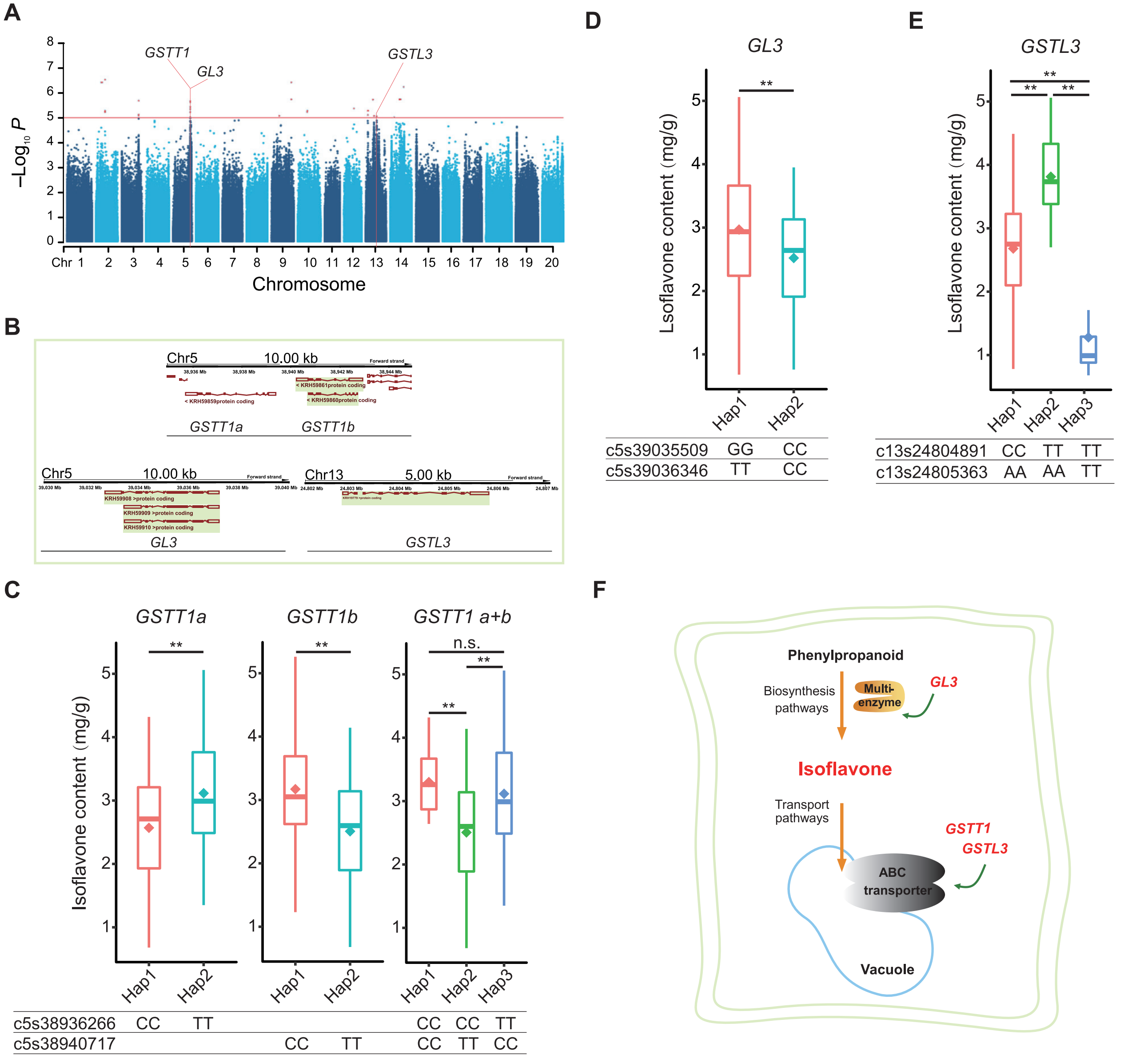

Figure 3 Three genes associated with soybean isoflavone content identified by GWAS

A. Manhattan plot and candidate genes for the soybean isoflavone content. **B.** Chromosome location and transcript structure of the candidate genes. **C.** Soybean isoflavone content distribution for the haplotypes of *GSTT1*. **D.** Soybean isoflavone content distribution for the haplotypes of *GL3*. **E.** Soybean isoflavone content distribution for the haplotypes of *GSTL3*. **F.** Diagram of soybean isoflavone synthesis and transport and the roles of candidate genes detected by GWAS. *, $P < 0.05$; **, $P < 0.01$; n.s., not significant. GWAS, genome-wide association study; Hap, haplotype.

traits. Furthermore, all SAGs and selective sweep regions for all traits were compared, revealing that approximately 12% of the SAGs were located in the selected sweep regions, which experienced artificial selection (Table S9). Of all the SAGs located in selective sweep regions, about 55% were related to yield traits, 36% were related to protein traits, and less than 10% were related to other traits (Figure 4H).

CYP85A2 was associated with both architecture- and yield-related traits

One SAL was located on chromosome 18, which was associated with six traits, including plant height, main stem number, stem strength, lodging, podding habit, and seed weight per plant. Interestingly, these traits included both architecture- and yield-related traits. A cytochrome P450 family gene named *CYP85A2* was located within a 4.37 kb region of this SAL (Figure 5A and B). The association of *CPY85A2* with the architecture- and yield-related traits in soybean was a novel finding. We also observed that a nonsynonymous mutation site c18s55526062 was involved in producing two haplotypes. Haplotype 1 with a CC genotype had a dwarf plant height, a low main stem node number, a high stem strength, and a low lodging rate. When plants produced mostly limited or semi-limited pods, their seed weight per plant was also found

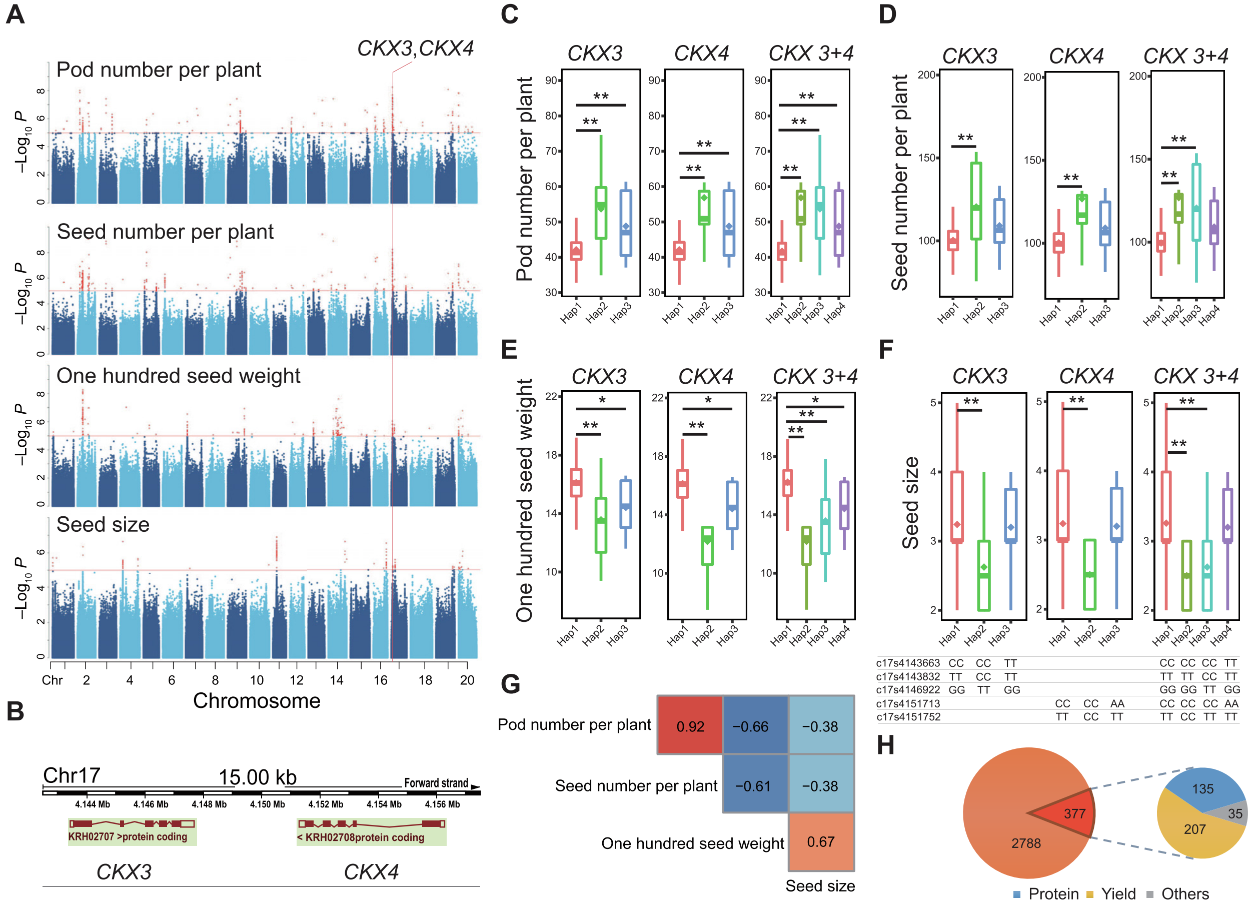

Figure 4 *CKX3* was associated with soybean yield-related traits
A. Manhattan plot of four yield-related traits (pod number per plant, seed number per plant, one hundred seed weight, and seed size) and the candidate *CKX* genes. **B.** Chromosome location and transcript structure of *CKX3* and *CKX4*. **C.** Pod number per plant distribution for the haplotypes of the *CKX* genes. **D.** Seed number per plant distribution for the haplotypes of the *CKX* genes. **E.** One hundred seed weight distribution for the haplotypes of the *CKX* genes. **F.** Seed size distribution for the haplotypes of the *CKX* genes. **G.** Phenotype correlation of four yield-related traits. **H.** Statistics of the SAGs located in selective sweep regions and their distributions for different trait categories. *, $P < 0.05$; **, $P < 0.01$.

to increase (Figure 5C). Phenotypically, plant height was positively correlated with main stem node number (0.95), while stem strength and lodging were negatively correlated (–0.81), showing a trend consistent with the genotype (Figure 5D). The CC genotype of c18s55526062 is a dominant genotype, which is useful when designing an ideal plant type and increasing soybean yield.

Construction of a complex phenotype–gene network using different phenotypes coupled with hub gene modules

Based on the in-depth exploration of the GWAS results, one trait was found to be associated with multiple genes and vice versa. At the same time, a complex network between various phenotypes and genes was also found due to the widespread protein-level interactions between genes. To explore this further, a functional mutation-based haplotype test was performed to screen SAGs in all SALs for all traits. Then, a phenotype–gene network was constructed, including 34 traits and 853 SAGs (**Figure 6**). At the trait level, they were divided into six categories, namely architecture, color, oil, isoflavone, protein, and yield. At the gene level, besides the six categories, a mixed category emerged in which genes associated with more than one trait category. Traits in the same category were closely linked within the entire network. However, some trait categories were also linked with each other, such as yield, oil, protein, and color, and they were all closely linked to architecture through common SAGs. This suggested subtle relationships between architecture and other trait categories. In this genetic network, 6 trait categories were linked through 15 hub nodes containing 367 genes (Table S10). The largest hub was *Hub Architecture 1* (*HA1*). The genes in this hub were associated with only two or more architecture-related traits. Unlike *HA1*, the genes in the *HA2* node were not only associated with two or more architecture-related traits but also had protein interactions with other genes. Multiple yield-related traits were associated with the *Hub Yield 1* (*HY1*) node, containing *CKX3*, while the *Hub Mixed 4* (*HM4*) node, containing *CYP85A2*, was connected with architecture- and yield-related traits.

Discussion

In this study, 250 representative landrace and cultivar soybean accessions were deeply sequenced. It is novel in evaluating the

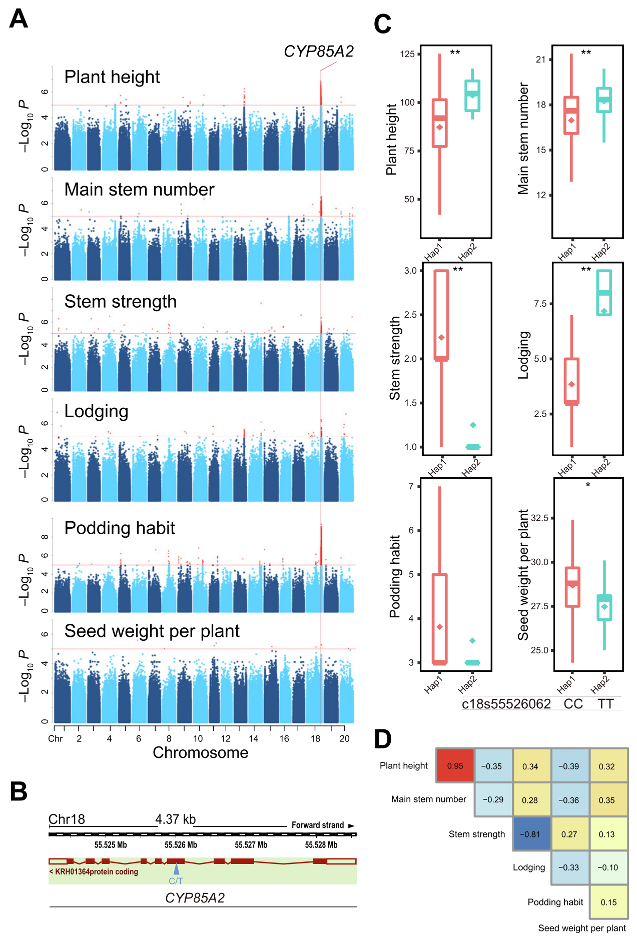

Figure 5 *CYP85A2* was associated with soybean architecture and yield-related traits

A. Manhattan plot of six architecture- and yield-related traits (plant height, main stem number, stem strength, lodging, podding habit, and seed weight per plant) and the candidate gene *CYP85A2*. **B.** Chromosome location and transcript structure of *CYP85A2*. **C.** Trait distribution for the haplotypes of *CYP85A2*. **D.** Phenotype correlation of the six traits. *, $P < 0.05$; **, $P < 0.01$.

genetic structure of European soybean varieties through population genetics and GWAS analyses. Novel candidate genes related to seed isoflavone content, yield, and architecture traits were identified. Moreover, a soybean phenotype–gene interaction network was constructed, and evidence of the improvement in soybean yield-related traits at the molecular level was found.

A total of ~ 3 Tb pair-end reads and 6 MB SNPs were obtained. The maximum sequencing depth of a single accession was 22.5×, with an average depth of 11× (higher than those in previous soybean resequencing studies [2–4]). Moreover, 84% of the accessions were sequenced for the first time, providing new data for soybean genome research. Previous soybean research mainly focused on varieties from Asia and North America but not from Europe [3,4]. This study completed the resequencing of 26 European accessions and, for the first time, outlined a breeding history of the European soybean. We found that European soybean cultivars had higher genetic diversities and lower breeding levels than North American cultivars. Both European and American soybean cultivars might have been introduced from different ancestors in China. This theory was based on the following findings: a small population difference between European cultivars and Chinese landraces and between American cultivars and Chinese cultivars, but a large population difference between American and European cultivars (Figure 2G, Figure S2). The findings were consistent with the current hypothesis that soybean originated in China; they showed that ancestral components from the area of origin were the most complex. This study showed that the heterozygosity rates of most accessions were less than 0.2, except for four accessions with higher heterozygosity caused by their complex ancestral compositions (Table S3). Further combination analysis of the selective sweep and GWAS revealed that the artificial selection of soybean at the phenotypic level was consistent with that at the genomic level. Genomic regions associated with yield and quality traits were more likely to experience artificial selection. This might reflect the yield- and quality-directed artificial selection of soybean breeding at the genetic level. Furthermore, we found evidence of functional mutations under artificial selection for a candidate gene *CKX3* related to multiple yield traits. This study provides valuable information for marker-assisted selection, which is vital for the improvement of soybean breeding.

Isoflavone is a secondary metabolite produced via phenylpropane metabolic pathways in higher plants. Isoflavone is associated with plant stress resistance, defense against microbial and insect infection, promotion of rhizobium chemotaxis, and development of rhizome and nitrogen fixation in plants. It also provides health benefits to humans, such as reducing the incidence of cancer and cardiovascular diseases and regulating the immune response [15]. Therefore, increasing the seed isoflavone content of soybean can improve its nutritional and health benefits. However, few genome-wide studies have investigated the molecular mechanism regulating the soybean isoflavone content. Isoflavone is synthesized in the cytoplasm, but it cannot be accumulated in the cytoplasm due to its cell cytotoxicity and must be continuously transported to vacuoles for storage. Therefore, the isoflavone content mainly depends on two factors: synthesis efficiency and transport efficiency [16]. The transcription factor GL3 is a bHLH family member that can form the MYB–bHLH–WD40 complex with two other transcription factors (MYB and WD40) to jointly regulate the synthesis of flavonoids and anthocyanin in plants [17]. GST can bind with glutathione to form an ABC transporter to transport and catalyze the entry of flavonoids into vacuoles for accumulation [16]. In this study, four novel genes associated with the isoflavone content were identified. These genes included *GL3*, which participated in regulating multi-enzyme systems from the phenylpropanoid pathway to the isoflavone biosynthesis pathway, and two *GST* genes *GSTT1* and *GSTL3*, which facilitated the transport of isoflavone from the cytoplasm to vacuoles (Figure 3F). In addition, many other genes were observed in the SALs, such as cation/H+ exchanger 20 (*CAX20*), pyrophosphorylase 4 (*PPa4*), actin-depolymerizing factor 7 (*ADF7*), and four genes encoding a mitochondrial substrate carrier family protein, a myosin heavy chain-related protein, an ATP synthase alpha/beta family protein, and a protein kinase superfamily protein, respectively (Table S8); they were all related to isoflavone transport. This over-representation of transport-related genes further suggested that the accumulation

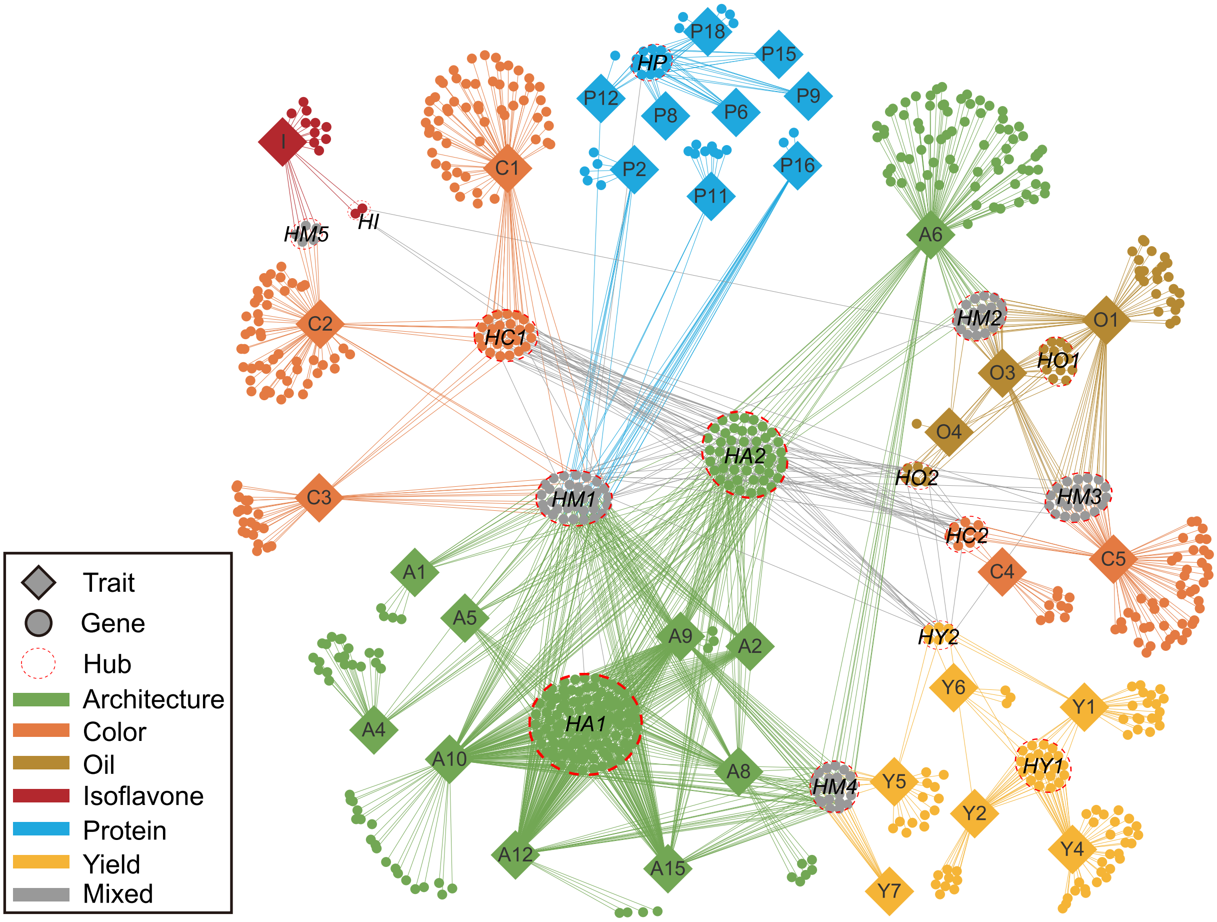

Figure 6 Phenotype–gene association/interaction network for six trait categories in soybean
Traits are represented as solid rhombuses, genes as solid circles, and hubs as hollow ellipses. Six trait categories, their associated genes, and the links between them are colored accordingly; genes associated with more than one trait category are colored in gray. Genes with protein–protein interactions are linked with gray lines. *HA*, *Hub Architecture*; *HY*, *Hub Yield*; *HM*, *Hub Mixed*; *HI*, *Hub Isoflavone*; *HC*, *Hub Color*; *HO*, *Hub Oil*; *HP*, *Hub Protein*.

of soybean isoflavone was related to its transport to the vacuole. In conclusion, the soybean isoflavone content is not determined merely by one or several genes or loci but by a multiple gene system involved in synthesis, regulation, transport, and storage.

Other novel candidate genes, such as *CKX3*, were associated with multiple yield-related traits. This study also found for the first time that *CYP85A2* was associated with multiple architecture- and yield-related traits in soybean. Cytokinin promotes cell division and plant growth, and *CKX* is one of the key enzymes in cytokinin metabolism. A functional variation in the *CKX* gene may affect the cytokinin metabolism, thus affecting grain yield and related traits. A number of studies on *Arabidopsis thaliana*, rice, and other crops have shown that mutations or reduced expression levels of the *CKX* family genes are related to a decrease in seed setting rate and an increase in seed weight [18,19]. *CYP85A2* is involved in the brassinosteroid (BR) biosynthesis pathway in *A. thaliana* and converts 6-deoxocastasterone into castasterone, which is followed by the conversion of castasterone into brassinolide [20]. BRs are broad-spectrum plant growth regulators playing an important role in plant growth and development, as well as in biological and abiotic stress responses [21]. Mutations in *CYP85A2* led to increased production of the dwarf phenotype [22], and overexpression of the *CYP85A* family gene resulted in increases in BR content, biomass, plant height, plant fresh weight, and fruit yield [23]. These results showed that *CKX3* and *CYP85A2* may affect soybean yield- and architecture-related traits through different molecular mechanisms. The potential effect of functional mutations in these genes on phenotypes was further confirmed by the haplotype tests. However, further functional verification of these genes is necessary to verify whether these candidate genes and functional mutations are the true cause of phenotypic differences. Multiple methods, such as construction of isolated populations, transgene, gene knockout, gene editing, and expression verification, can be used for this purpose. In this study, expression verification was performed in seedlings with different haplotypes/phenotypes for six genes *GL3*, *GSTL3*, *GSTT1b*, *CKX3*, *CKX4*, and *CYP85A2*. The results showed that, except for *CKX4* (no expression was detected), the other five genes were differentially expressed in seedlings with different haplotypes/phenotypes. The expression levels of *GL3*, *GSTL3*, and *GSTT1b* were significantly higher in the seedlings with high isoflavone content than those with low isoflavone content ($P < 0.05$, *t*-test). The expression level of *CKX3* was significantly higher in the seedlings with high-yield phenotype than those with low-yield phenotype ($P < 0.05$, *t*-test; Figure S55).

The highest goal of plant breeding is to aggregate many desired traits into a single genome. Breeders need to select and improve multiple related traits simultaneously. However, since multiple traits are interrelated, it is possible that when screening for a favorable trait, an unfavorable one is also selected. Understanding the genetic network behind different traits can help breeders increase breeding efficiency. Although soybean genetic networks for multiple agronomic traits have been established at the locus level [4], a new phenotype–gene network including 34 traits and 853 genes was built in this study. This network reflects the relationships between phenotypes and genes more directly than the previous phenotype–SAL network and is more conducive to discoverying important candidate genes. For example, the *Hub Mixed 1* (*HM1*) node is associated with two or more trait types (architecture, color, or protein). Specifically, the *HBT* gene in the *HM1* node is associated with six architecture-related traits (branch number, main stem number, plant height, stem strength, lodging, and podding habit) and four protein-related traits (phenylalanine content, isoleucine content, tyrosine content, and glycine content). The *HBT* gene belongs to the *CDC27b* gene family and is involved in cell cycle regulation, which is related to cell development and division [24]. Therefore, soybean architecture is likely affected by *HBT*; however, its relationship with the amino acid content is unclear. Leaf shape is known to affect photosynthesis efficiency, followed by carbohydrate accumulation and, consequently, oil accumulation; in our network, the *HM2* node, containing *FAD2*, also relates oil content to leaf shape [25]. Oil-related traits and seed coat luster-related traits have experienced parallel selection during bean domestication [26]; the *HM3* node also connects oil-related traits and seed coat luster-related traits. Anthocyanin synthesis and isoflavone synthesis share part of their metabolic pathways, and the *HM5* node connects color-related traits and isoflavone content as well. This phenotype–gene network may surpass the previous phenotype–SAL network in terms of candidate gene selection, which is also beneficial to polymerization breeding programs. For example, breeders can achieve polymerization breeding by directly selecting a favorable gene (such as *CYP85A2*) in hub *HM4*, which is related to both yield and architecture traits and eliminates the confusion of other adverse genes located in the same SAL. Furthermore, the architecture-related traits, which centrally connect various other trait categories, have the most extensive connectivity. In other words, numerous relationships exist between architecture-related traits and other trait categories in the phenotype–gene network (Figure 6), suggesting that some candidate genes related to architecture traits may also be related to other trait types. This may provide theoretical support and practical guidance for parallel selection breeding and promote "ideotype" breeding in soybean. The next step is to conduct more in-depth functional investigations on genes with a potential application value, such as *CKX3* and *CYP85A2*. This would help promote the design and breeding process of soybean varieties with a higher yield and quality. Overall, the present study is conducive to promoting soybean genome functional research and genomic breeding.

Materials and methods

Plant materials and phenotyping

A total of 250 soybean accessions were analyzed in this study, which was provided by the National Crop Germplasm Resources Platform, Institute of Crop Genetics, Institute of Crop Sciences, Chinese Academy of Agricultural Sciences. All materials were planted and phenotyped at three locations: the Gongzhuling experimental site in the Jilin Academy of Agricultural Sciences, China (north latitude 43.51°, east longitude 124.80°), the Harbin experimental site in the Heilongjiang Academy of Agricultural Sciences, China (north latitude 45.68°, east longitude 126.61°), and the Chifeng experimental site in the Agricultural Science Institute in Inner Mongolia, China (north latitude 42.27°, east longitude 118.90°) in late April of 2008, 2009, and 2010, respectively. The grain protein content was measured using the Kjeldahl method from the National Food Safety Standard GB5009.5-2010, China (GB/T 5009.5-2010 National food safety standard—Determination of protein in foods), while the grain fatty acid content was determined using the Soxhlet extraction method from the National Food Safety Standard GB/T5512-2008, China (GB/T 5512-2008 Inspect of grain and oilseeds—Determination of crude fat content in grain). The amino acid content was determined using high-performance liquid chromatography (HPLC; Catalog No. S433D, Seckam, Germany) following a previous amino acid determination method from the National Food Safety Standard GB/T 18246-2000, China (GB/T 18246-2000 Determination of amino acids in feeds). The grain isoflavone content was determined using HPLC following the National Food Safety Standard GB/T23788-2009, China (GB/T 23788-2009 Determination of soybean isoflavone in health-care food-High-performance liquid chromatography). Finally, the phenotypic data were integrated by the BLUP method using R [27] to remove environmental effects and obtain stable genetic phenotypes. The seeds were planted in CLC-BIV-M/CLC404-TV (MMM, Germany) at 20 °C (with 12 h day/12 h night) and relative humidity of 60%–80% till the six-leaf stage (about 2-week-old). Two-week-old seedlings (24 °C, 12 h day/12 h night cycle) were used for qRT-PCR validation.

DNA preparation and sequencing

The genomic DNA for all soybean accessions was extracted from soybean leaves after 3 weeks of growth. DNA was extracted using the cetyltrimethylammonium bromide method [28]. The library for each accession was constructed with an insert size of approximately 500 bp following the manufacturer's protocols (Illumina, CA). All soybean accessions were sequenced, and paired-end 150 bp reads were produced using an Illumina NovaSeq 6000 sequencer at the BerryGenomics Company (http://www.berrygenomics.com/; Beijing, China).

Total RNA extraction, cDNA synthesis, and qRT-PCR analysis

Total RNA was isolated from each sample using TRIzol reagent (Invitrogen, Nottingham, UK) following the manufacturer's protocols. The purified RNA was stored at −80 °C until subsequent analyses. The first-strand cDNA synthesis was performed using M-MLV reverse transcriptase following the manufacturer's protocols (TaKaRa, Shiga, Japan). qRT-PCR was performed using an SYBR Premix Ex Taq Kit (TaKaRa) and a real-time PCR machine (Catolog No. CFX96, Bio-Rad, CA) following the manufacturer's protocols. The procedure used for qRT-PCR was 95 °C for 10 min, followed by 38 cycles of 15 s at 95 °C and 60 s at 61–62 °C. *β-actin* was used as the reference gene for analyzing the relative expression patterns of mRNA. The reactions were carried out with three biological replicates, with at least two technical replicates for each sample. The data were analyzed as previously described [29]. Finally, the data of three biological replicates were presented as mean ± SD.

Mapping, variant calling, and annotation

Raw paired-end resequencing reads were first cleaned by removing reads with adaptors, reads of low quality, and reads with "N"s. The high-quality clean reads were subsequently mapped to the soybean reference genome (Williams 82 assembly v2.1) with BWA [30]. Statistical analyses of mapping rate and genomic coverage of clean reads were performed using in-house scripts. The Speedseq pipeline [31] was used for SNP and InDel calling, and VCFtools [32] was used for genotype filtering. Missing genotypes were imputed and phased through a localized haplotype clustering algorithm implemented using Beagle v3.0 [33]. Variant annotation was performed using ANNOVAR [34] against the soybean gene model set v2.1.42. After annotation, SNPs and InDels were categorized into exonic, intronic, intergenic, splicing, 5′-UTRs, 3′-UTRs, upstream, and downstream. Exonic SNPs were further categorized into synonymous, nonsynonymous, stop gain, and stop loss. Exonic InDels were further categorized into frameshift, non-frameshift, stop gain, and stop loss.

Population structure analysis

Approximately 6 MB SNPs from the 250 soybean accessions were concatenated for constructing a phylogenetic tree. The phylogenetic tree was constructed with MegaCC using an NJ algorithm with a pairwise gap deletion method for 100 bootstrap replications [35]. The output was displayed using the iTOL [36] web tool. With the whole-genome genotype as input, a PCA was performed using flashPCA [37], and the first two eigenvectors were plotted. A population admixture analysis with $K = 2$ to $K = 5$ was performed to infer the admixture of ancestors using fastSTRUCTURE [38].

Genetic diversity analysis

Genetic diversity analysis was performed using the scripts provided by the SR4R database [39]. LD analyses for each subpopulation were performed using PLINK [40] by calculating the correlation coefficient (r^2) of any two SNP pairs in one chromosome. An LD decay plot was drawn using the average r^2 value for the distance from 0 to 1000 kb. Pairwise IBS calculations were also performed using PLINK, and a distance matrix was generated for each subpopulation. Population genetic diversities were measured using VCFtools [32] by calculating $\theta\pi$ and *Fst*. $\theta\pi$ was used to measure the genetic diversity of each subpopulation, while *Fst*, plus the AFD plot (which was generated by in-house scripts), was used to measure genetic diversity between subpopulations. In addition, sliding window calculations of r^2, $\theta\pi$, *Fst*, and Tajima's *D* values were performed for genome-wide displays of soybean genetic diversities with a 100 kb window and a 10 kb step.

Selective sweep analysis

Two methods were used to detect selective sweep regions across the soybean genome: Tajima's *D* combined with $\theta\pi$ and *Fst* combined with $\theta\pi$ ratios. First, a genome-wide sliding window calculation of $\theta\pi$, *Fst*, and Tajima's *D* (with a 100 kb window and a 10 kb step) was performed on landraces, cultivars, and the whole population, respectively. Second, the top 5% of the Tajima's *D* and $\theta\pi$ windows for the whole population were selected. In addition, the top 5% of the *Fst* and $\theta\pi$ ratio windows for the landraces versus cultivars were also selected. Third, the selected windows using these two methods were merged to form the final selective sweep regions. ROH analyses for each accession were performed using PLINK [40] by setting the minimum ROH length to 300 kb.

GWAS and detection of SALs

The association analysis for each trait on each SNP with a MAF larger than 0.05 was performed using a single-locus MLM implemented in GEMMA [41] (which corrects for confounding effects due to the population structure and the relatedness matrix). The GWAS results were displayed using a Manhattan plot and a QQ-plot created with the R package CMplot [42]. A clump-based method implemented in PLINK [40] was used to reduce a false peak and detect real SALs. The *P*-value cutoff was set to 1×10^{-5} to first uncover significantly associated SNPs. Following this, for each significantly associated SNP, the region was regarded as a potential SAL if more than 10 SNPs within a 100 kb distance had *P* values smaller than 1×10^{-4}. Finally, all overlapping SALs were merged to generate final SAL sets, and the SNP with the smallest *P* value in a SAL was defined as a peak.

Detection of SAGs

Usually, tens of genes are present in a SAL; hence, it is difficult to determine which genes are truly associated with traits. An improved functional mutation-based haplotype test method was used in this study for SAG discovery in SALs. As most variants within a gene are nonfunctional, the amino acid sequence and function of the gene do not change. Only a few variants have the potential to change the amino acid sequence of a gene, such as nonsynonymous SNPs, frameshift InDels, and variants in splicing sites, promoter regions, start codons, and stop codons. These combined functional mutations can only produce two or three different gene haplotypes. It is possible to test the relationship between gene haplotypes and traits. If they are significantly associated, then the gene is also most likely associated with the trait, which is how a SAG is defined. In this study, Welch's test was used for a two-group haplotype test, and a Tukey's test was used for a multiple-group haplotype test to detect SAGs. The functional annotation of SAGs was directly retrieved from SoyBase [43].

Network construction

Of all the genes located in the SALs, the most significant SAGs with $P < 1 \times 10^{-5}$, and their corresponding traits, were retained to build the phenotype–gene network for soybean. Protein–protein interaction information for soybean was retrieved from the STRING database [44] and mapped to the soybean genes using BLAST [45]. The construction, visualization, and exploration of the network were performed using Cytoscape [46].

Code availability

The bioinformatics analysis scripts used in this study can be downloaded through https://github.com/yjthu/GPB_250SoyReseq.

Data availability

The raw sequence data reported in this study have been deposited in the Genome Sequence Archive [47] at the National Genomics Data Center, Beijing Institute of Genomics, Chinese Academy of Sciences / China National Center for Bioinformation (GSA: CRA002552), and are publicly accessible at https://ngdc.cncb.ac.cn/gsa. The variation data are publicly accessible at the Genome Variation Map database (GVM: GVM000076), and are publicly accessible at https://ngdc.cncb.ac.cn/gvm [48].

CRediT author statement

Chunming Yang: Resources, Investigation, Validation. **Jun Yan:** Methodology, Formal analysis, Writing - original draft, Writing - review & editing. **Shuqin Jiang:** Formal analysis. **Xia Li:** Investigation, Validation. **Haowei Min:** Conceptualization, Supervision, Formal analysis, Writing - review & editing. **Xiangfeng Wang:** Conceptualization, Supervision, Writing - review & editing. **Dongyun Hao:** Conceptualization, Supervision, Writing - review & editing. All authors have read and approved the final manuscript.

Competing interests

The authors declare no competing financial interests.

Acknowledgments

This study was supported by grants from the Agricultural Science and Technology Innovation Project, Jilin Province, China (Grant No. CXGC2017ZY027), the Program of Accurate Identification and Display of Soybean Germplasm, China [Grant Nos. NB08-2130315-(25-31)-06, NB07-2130315-(25-30)-06, NB06-070401-(22-27)-05, and NB2010-2130315-25-05], and the Chinese Universities Scientific Fund. We are grateful to Prof. Lijuan Qiu for her agreement of using the 250 soybean accessions from her laboratory at the China Academy of Agricultural Sciences. We appreciate Dr. Zhangxiong Liu of China Academy of Agricultural Sciences for the technical guidance in soybean phenotypic characterization. We also thank Yunshan Wei (Inner Mongolia Academy of Agriculture & Animal Husbandry Sciences, China) and Shuhong Wei and Qiang Wang (Heilongjiang Academy of Agricultural Sciences, China) for partial phenotypic characterization of the soybean population used in this study.

Supplementary material

Supplementary data to this article can be found online at https://doi.org/10.1016/j.gpb.2021.02.009.

ORCID

ORCID 0000-0001-7071-500X (Chunming Yang)
ORCID 0000-0002-3806-6457 (Jun Yan)
ORCID 0000-0003-4959-931X (Shuqin Jiang)
ORCID 0000-0001-8162-2335 (Xia Li)
ORCID 0000-0003-3391-7379 (Haowei Min)
ORCID 0000-0002-6406-5597 (Xiangfeng Wang)
ORCID 0000-0001-8550-0992 (Dongyun Hao)

References

[1] Sedivy EJ, Wu F, Hanzawa Y. Soybean domestication: the origin, genetic architecture and molecular bases. New Phytol 2017;214:539–53.

[2] Lam HM, Xu X, Liu X, Chen W, Yang G, Wong FL, et al. Resequencing of 31 wild and cultivated soybean genomes identifies patterns of genetic diversity and selection. Nat Genet 2010;42:1053–9.

[3] Zhou Z, Jiang Y, Wang Z, Gou Z, Lyu J, Li W, et al. Resequencing 302 wild and cultivated accessions identifies genes related to domestication and improvement in soybean. Nat Biotechnol 2015;33:408–14.

[4] Fang C, Ma Y, Wu S, Liu Z, Wang Z, Yang R, et al. Genome-wide association studies dissect the genetic networks underlying agronomical traits in soybean. Genome Biol 2017;18:161.

[5] Yan J, Lv S, Hu M, Gao Z, He H, Ma Q, et al. Single-molecule sequencing assists genome assembly improvement and structural variation inference. Mol Plant 2016;9:1085–7.

[6] Wang W, Mauleon R, Hu Z, Chebotarov D, Tai S, Wu Z, et al. Genomic variation in 3,010 diverse accessions of Asian cultivated rice. Nature 2018;557:43–9.

[7] Yang N, Liu J, Gao Q, Gui S, Chen L, Yang L, et al. Genome assembly of a tropical maize inbred line provides insights into structural variation and crop improvement. Nat Genet 2019;51:1052–9.

[8] Schmutz J, Cannon SB, Schlueter J, Ma J, Mitros T, Nelson W, et al. Genome sequence of the palaeopolyploid soybean. Nature 2010;463:178–83.

[9] Nielsen R. Molecular signatures of natural selection. Annu Rev Genet 2005;39:197–218.

[10] Purfield DC, McParland S, Wall E, Berry DP. The distribution of runs of homozygosity and selection signatures in six commercial meat sheep breeds. PLoS One 2017;12:e0176780.

[11] Crowell S, Korniliev P, Falcão A, Ismail A, Gregorio G, Mezey J, et al. Genome-wide association and high-resolution phenotyping link *Oryza sativa* panicle traits to numerous trait-specific QTL clusters. Nat Commun 2016;7:10527.

[12] Yano K, Yamamoto E, Aya K, Takeuchi H, Lo PC, Hu L, et al. Genome-wide association study using whole-genome sequencing rapidly identifies new genes influencing agronomic traits in rice. Nat Genet 2016;48:927–34.

[13] Meng S, He J, Zhao T, Xing G, Li Y, Yang S, et al. Detecting the QTL-allele system of seed isoflavone content in Chinese soybean landrace population for optimal cross design and gene system exploration. Theor Appl Genet 2016;129:1557–76.

[14] Zhang J, Wang X, Lu Y, Bhusal SJ, Song Q, Cregan PB, et al. Genome-wide scan for seed composition provides insights into soybean quality improvement and the impacts of domestication and breeding. Mol Plant 2018;11:460–72.

[15] Messina M. A brief historical overview of the past two decades of soy and isoflavone research. J Nutr 2010;140:1350S–4S.

[16] Braidot E, Zancani M, Petrussa E, Peresson C, Bertolini A, Patui S, et al. Transport and accumulation of flavonoids in grapevine (*Vitis vinifera* L.). Plant Signal Behav 2008;3:626–32.

[17] Xu W, Dubos C, Lepiniec L. Transcriptional control of flavonoid biosynthesis by MYB–bHLH–WDR complexes. Trends Plant Sci 2015;20:176–85.

[18] Li J, Nie X, Tan JLH, Berger F. Integration of epigenetic and genetic controls of seed size by cytokinin in *Arabidopsis*. Proc Natl Acad Sci U S A 2013;110:15479–84.

[19] Ashikari M, Sakakibara H, Lin S, Yamamoto T, Takashi T, Nishimura A, et al. Cytokinin oxidase regulates rice grain production. Science 2005;309:741–5.

[20] Kim TW, Hwang JY, Kim YS, Joo SH, Chang SC, Lee JS, et al. *Arabidopsis* CYP85A2, a cytochrome P450, mediates the Baeyer-Villiger oxidation of castasterone to brassinolide in brassinosteroid biosynthesis. Plant Cell 2005;17:2397–412.

[21] De Bruyne L, Höfte M, De Vleesschauwer D. Connecting growth and defense: the emerging roles of brassinosteroids and gibberellins in plant innate immunity. Mol Plant 2014;7:943–59.

[22] Kwon M, Fujioka S, Jeon JH, Kim HB, Takatsuto S, Yoshida S, et al. A double mutant for the *CYP85A1* and *CYP85A2* genes of *Arabidopsis* exhibits a brassinosteroid dwarf phenotype. J Plant Biol 2005;48:237–44.

[23] Northey JG, Liang S, Jamshed M, Deb S, Foo E, Reid JB, et al. Farnesylation mediates brassinosteroid biosynthesis to regulate abscisic acid responses. Nat Plants 2016;2:16114.

[24] Perez-Perez JM, Serralbo O, Vanstraelen M, Gonzalez C, Criqui MC, Genschik P, et al. Specialization of CDC27 function in the *Arabidopsis thaliana* anaphase-promoting complex (APC/C). Plant J 2008;53:78–89.

[25] Dar AA, Choudhury AR, Kancharla PK, Arumugam N. The *FAD2* gene in plants: occurrence, regulation, and role. Front Plant Sci 2017;8:1789.

[26] Zhang D, Sun L, Li S, Wang W, Ding Y, Swarm SA, et al. Elevation of soybean seed oil content through selection for seed coat shininess. Nat Plants 2018;4:30–5.

[27] Liu XQ, Rong JY, Liu XY. Best linear unbiased prediction for linear combinations in general mixed linear models. J Multivariate Anal 2008;99:1503–17.

[28] Murray MG, Thompson WF. Rapid isolation of high molecular weight plant DNA. Nucleic Acids Res 1980;8:4321–6.

[29] Livak KJ, Schmittgen TD. Analysis of relative gene expression data using real-time quantitative PCR and the $2^{-\Delta\Delta C_T}$ method. Methods 2001;25:402–8.

[30] Li H, Durbin R. Fast and accurate long-read alignment with Burrows-Wheeler transform. Bioinformatics 2010;26: 589–95.

[31] Chiang C, Layer RM, Faust GG, Lindberg MR, Rose DB, Garrison EP, et al. SpeedSeq: ultra-fast personal genome analysis and interpretation. Nat Methods 2015;12:966–8.

[32] Danecek P, Auton A, Abecasis G, Albers CA, Banks E, DePristo MA, et al. The variant call format and VCFtools. Bioinformatics 2011;27:2156–8.

[33] Browning SR, Browning BL. Rapid and accurate haplotype phasing and missing-data inference for whole-genome association studies by use of localized haplotype clustering. Am J Hum Genet 2007;81:1084–97.

[34] Wang K, Li M, Hakonarson H. ANNOVAR: functional annotation of genetic variants from high-throughput sequencing data. Nucleic Acids Res 2010;38:e164.

[35] Kumar S, Stecher G, Peterson D, Tamura K. MEGA-CC: computing core of molecular evolutionary genetics analysis program for automated and iterative data analysis. Bioinformatics 2012;28:2685–6.

[36] Letunic I, Bork P. Interactive Tree Of Life (iTOL) v4: recent updates and new developments. Nucleic Acids Res 2019;47:W256–9.

[37] Abraham G, Inouye M. Fast principal component analysis of large-scale genome-wide data. PLoS One 2014;9:e93766.

[38] Raj A, Stephens M, Pritchard JK. fastSTRUCTURE: variational inference of population structure in large SNP data sets. Genetics 2014;197:573–89.

[39] Yan J, Zou D, Li C, Zhang Z, Song S, Wang X. SR4R: an integrative SNP resource for genomic breeding and population research in rice. Genomics Proteomics Bioinformatics 2020;18:173–85.

[40] Chang CC, Chow CC, Tellier LC, Vattikuti S, Purcell SM, Lee JJ. Second-generation PLINK: rising to the challenge of larger and richer datasets. Gigascience 2015;4:7.

[41] Zhou X, Stephens M. Genome-wide efficient mixed-model analysis for association studies. Nat Genet 2012;44:821–4.

[42] Yin L, Zhang H, Tang Z, Xu J, Yin D, Zhang Z, et al. rMVP: a memory-efficient, visualization-enhanced, and parallel-accelerated tool for genome-wide association study. Genomics Proteomics Bioinformatics 2021;19:619–28.

[43] Grant D, Nelson RT, Cannon SB, Shoemaker RC. SoyBase, the USDA-ARS soybean genetics and genomics database. Nucleic Acids Res 2010;38:D843–6.

[44] Szklarczyk D, Morris JH, Cook H, Kuhn M, Wyder S, Simonovic M, et al. The STRING database in 2017: quality-controlled protein-protein association networks, made broadly accessible. Nucleic Acids Res 2017;45:D362–8.

[45] Camacho C, Coulouris G, Avagyan V, Ma N, Papadopoulos J, Bealer K, et al. BLAST+: architecture and applications. BMC Bioinformatics 2009;10:421.

[46] Shannon P, Markiel A, Ozier O, Baliga NS, Wang JT, Ramage D, et al. Cytoscape: a software environment for integrated models of biomolecular interaction networks. Genome Res 2003;13:2498–504.

[47] Chen T, Chen X, Zhang S, Zhu J, Tang B, Wang A, et al. The Genome Sequence Archive Family: toward explosive data growth and diverse data types. Genomics Proteomics Bioinformatics 2021;19:578–83.

[48] Song S, Tian D, Li C, Tang B, Dong L, Xiao J, et al. Genome Variation Map: a data repository of genome variations in BIG Data Center. Nucleic Acids Res 2018;46:D944–9.